Proc. Estonian Acad. Sci. Eng., 2003, **9**, 2, 126–136
https://doi.org/10.3176/eng.2003.2.04

Microstructural effects on wear of non-homogeneous hardmetal materials

Irina Hussainova and Mart Viljus

Department of Materials Technology, Tallinn Technical University, Ehitajate tee 5, 19086 Tallinn, Estonia; irhus@staff.ttu.ee

Received 28 November 2002, in revised form 14 March 2003

Abstract. Microstructure and composition of ceramic–metal alloys have been investigated using scanning electron microscope and energy-dispersive X-ray analysis. It is shown that microstructural variables play even more important role in the tribological performance of multiphase materials than the measured mechanical properties.

Key words: non-homogeneous materials, microstructure, tribology, SEM, X-ray analysis.

1. INTRODUCTION

Widespread use of ceramic–metal composites as materials for working elements of various equipment and machine parts is primarily due to their unique combination of desirable properties such as high hardness, strength, stiffness, wear, and corrosion resistance. However, until now there is no common understanding of damage processes of non-homogeneous materials.

As it is generally assumed, the wear behaviour of cermet materials is a direct function of both hardness and toughness [1]. Thus optimum wear behaviour is obtained when both these parameters are maximized. It has been observed that carbide particle size influences the abrasive and erosive wear rate [2,3]. Fine particles provide increased wear resistance at equivalent carbide particle volume fractions as compared with the coarse particles. In addition to grain size, porosity has also been shown to affect wear behaviour, with increased porosity leading to degradation in the wear resistance of cermets [4].

The fact that microstructural variables can influence wear behaviour is frequently overlooked in the literature. Moreover, these variables are not limited to the matrix grain size and porosity. Microstructure of the grain boundary and

composition play an important role in wear behaviour of non-homogeneous materials. In some alloys interfaces are the weak link causing brittle failure or grain boundary sliding, whereas in other materials they may be responsible for the strengthening by impeding dislocation movement. Segregation of solute elements or impurities to interfaces can be detrimental in some cases, but beneficial in other ones. Moreover, the stresses generated by boundary crystallization may influence the tribological behaviour of composites.

The present work considers the microstructural aspects related to wear resistance and investigates mechanisms of material removal of six carbide-based ceramic–metal composites.

2. MATERIALS

All materials investigated were produced through conventional press-and-sinter powder metallurgy. Selection of this technology was partly caused by the simplicity of incorporation of a hard phase into a metal phase through the blending of powders.

The cobalt content of the WC-Co hard metals tested was 8–20 wt %. The content of TiC carbides in TiC-based cermets investigated was 60–80 wt %. In Cr_3C_2-Ni composites the content of the metal binder was 15–30 wt %. The average grain size of carbide particles was 2.0–6.0 μm, porosity 0.1–0.2 vol% for all materials tested with the exception of chromium carbide based ones. The porosity of Cr_3C_2-Ni composites was about 2 vol%. An overview of the composition and mechanical characteristics of the composites examined in this study is presented in Table 1.

Table 1. Composition and mechanical properties of the composites tested

Grade	Carbide content, wt %	Composition and structure of the binder	Vickers hardness, *HV*	Density ρ, kg m^{-3}	Transverse rupture strength R_{TZ}, GPa	Modulus of elasticity *E*, GPa	Fracture toughness K_{IC}, MPa m$^{1/2}$
A1	92 WC	Co	1350	14500	2.3	650	13.0
A2	80 WC	Co	1030	13700	3.00	550	19.0
BS1	75 TiC	steel	1320	5460	1.8	300	15.0
BS2	60 TiC	steel	1000	5880	2.45	380	15.5
B1	80 TiC	Ni-Mo	1378	5500	1.08	400	11.5
B2	60 TiC	Ni-Mo	990	6040	1.32	380	18.5
C1	85 Cr_3C_2	Ni	1410	6970	0.9	340	9.8
C2	70 Cr_3C_2	Ni	980	7190	1.4	320	18.3

The densities of the samples were measured using the water immersion technique (Archimedes approach). Vickers hardness was determined with a micro-hardness tester using a 5 kg load. Fracture toughness was measured using indentation method developed by Evans et al. [5].

3. RESULTS AND DISCUSSION

3.1. Microstructure

Jeol 840A scanning electron microscope with LINK Analytical 10/95 series analyser was applied for microstructure observation and for the energy-dispersive X-ray microanalysis. Microstructure of the materials tested is shown in Fig. 1. The cobalt binder contracts during cooling, leaving the WC grains under compression [6]. It undergoes a transformation from metastable to stable phase during deformation and consequently has a high stacking fault level [6].

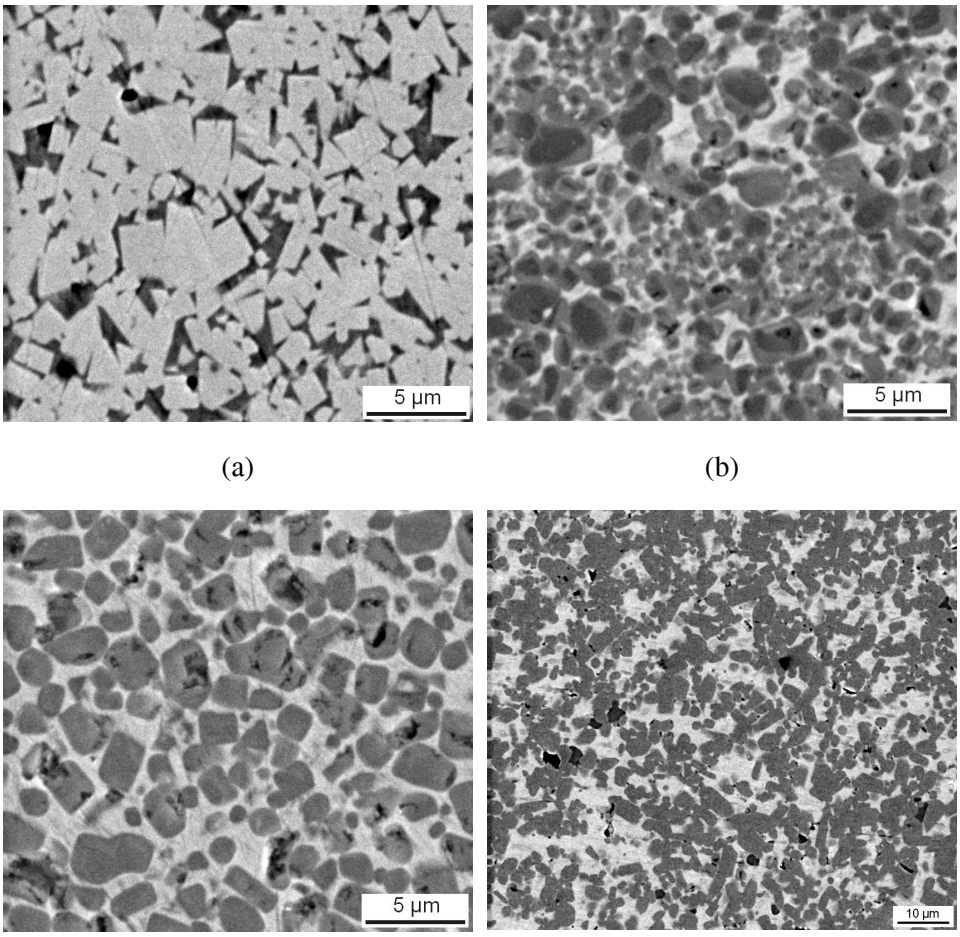

(a) (b)

(c) (d)

Fig. 1. SEM micrographs of ceramic–metal composites: (a) A2; (b) B1; (c) BS1; (d) C2 (see Table 1).

Re-precipitation onto TiC grains results in the typical cermet microstructure: core–rim structured hard grains surrounded by a tough metallic binder phase forming TiC-Mo_2C-Ni cermet structure (Fig. 1b). Unlike the angular shape of the tungsten carbide (Fig. 1a), the shape of TiC, when sintering in Ni(Mo), is rounded. Replacing 10 wt % of the Ni binder with Mo resulted in complete wetting (i.e., contact angle reaches 0 deg). The majority of the Mo is found within the carbide phase, forming the (Ti,Mo)C complex carbide. The hard phases, which are present in the material, consist of a core, rich in titanium carbide, and a molybdenum carbide rich shell; core–rim structured hard grains surrounded by a tough metallic binder phase form TiC-Mo_2C-Ni material (Fig. 2a). The outer and inner layers of the rim contain also some amount of Mo and only the very centre of the core shows no additions. Such a structure results in a decrease in the carbide phase continuity and an increase in the interphase bond strength. Because of the core–rim structure, there is no significant difference in mechanical properties at the interfaces. A small amount of micro-structural flaws such as voids, interphase debonding, and binder microcracks are observed on the TiC-NiMo surface.

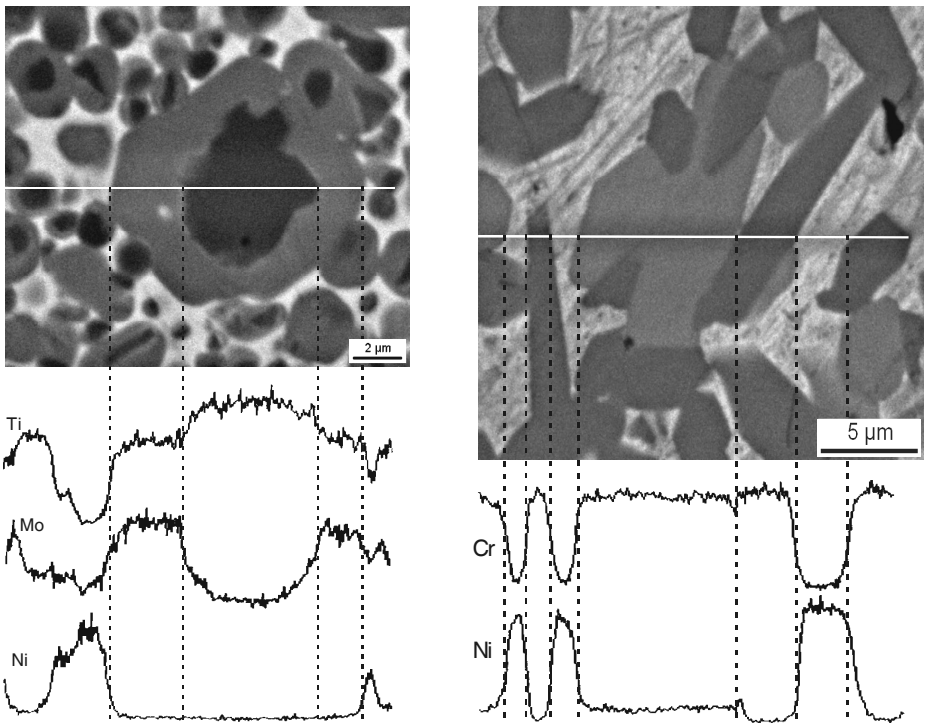

Fig. 2. X-ray image of B1 (a) and C1 (b).

Both the interphase debonding and the microcracks within the alloy binder show that large residual tensile stresses exist within the steel binder phase (Fig. 1c). Residual stresses in TiC-based cermets are caused by the difference in the thermal expansion behaviour of the two phases. A carbide skeleton structure with increased rigidity, following densification (increased carbide contiguity) is formed. As the material cools, residual stresses are generated. This can lead to nucleation and propagation of microcracks. The TiC-steel alloy microstructure develops by a continual process of dissolution and supersaturation of C in the Ti-C-Fe-Ni melt. Re-precipitation onto TiC grains does not result in the typical cermet core–rim microstructure. During sintering there is no complete wettability of TiC by Fe(Ni) liquid phase and as a result there are carbide–carbide grain boundaries forming "skeleton" structure.

The Cr_3C_2 grains in chromium carbide based materials are prismatic in shape and not surrounded completely by the binder phase (Fig. 1d). There is a significant amount of carbide–carbide contacts in the material. In Fig. 2b the X-ray linescan image of the 85% Cr_3C_2-15% Ni cermet is presented. The more interesting feature is lightly different composition of carbide grains. Two types of carbide grains can be seen with different gray color level (that indicates a different composition). Some of the carbide grains (the lighter ones) contain small quantities of nickel. The influence of the nickel-doped carbide grains on the mechanical properties of the alloy needs further investigation.

The dihedral angles are large and the extent of penetration of Ni is not significant at grain boundaries or at the particle junction. There is coalescence of adjacent grains and grain–grain interfacial energy may be twice greater than that of the grain–binder energy. It results in reduced strength of intergranular surfaces and improvement in conditions for intergranular cracks propagation.

As it can be seen from Fig. 1, the matrix grains in each of these materials have an anisotropic shape with certain size distribution. Since the grain size is undoubtedly an important factor in determining the wear behaviour of non-homogeneous materials, indication of the matrix grain size is necessary. Size distribution was conveniently measured with SEM using the back scattered electron mode. For this study, carbide grain size has been defined as the average of a minimum of 500 measured grain diameters and was in between 3.0 and 5.0 μm for ceramic–metal composites investigated.

3.2. Fracture morphology

SEM micrographs in Figs. 3 and 4 show the single impact craters generated by abrasive particles during the erosion test. Carbide particle fracture, interphase debonding, and microcracks within the binder can be seen. In all composites, extensive damage is observed in the matrix in all parts of the impact crater. However, the amount of damage in the hard skeleton increases from the edge of the crater to its centre. Since not many cracks in hard grains are observed, it is very likely that the carbide particles are fractured just beneath the eroded surface.

Evidence of subsurface cracking is seen in the SEM image of the cross-section in Fig. 5. In addition, material is extruded from the groove by impacting particles. It is easy to imagine that subsequent impact could detach this extruded material. Moreover, many grains near the crater are displaced that accumulates the additive grain–boundary strain.

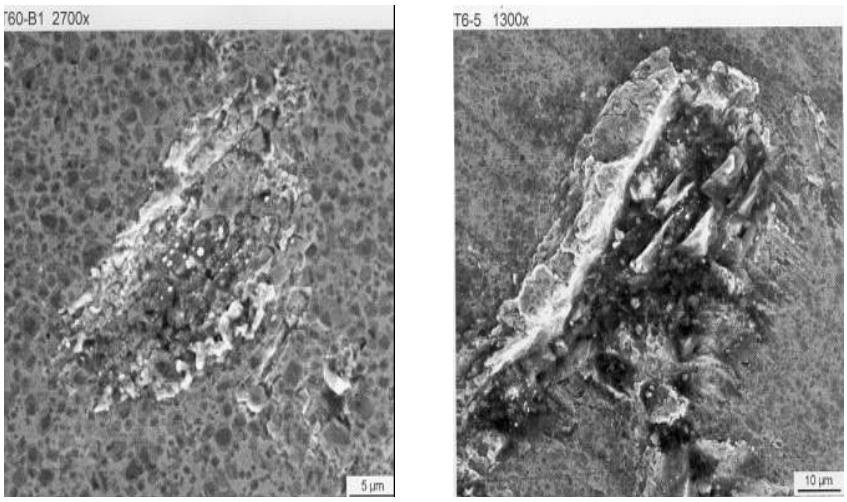

(a) (b)

Fig. 3. SEM micrographs of single impact crater produced in TiC-40%NiMo surface by a silica particle (a) and a silicon carbide particle (b). Particle velocity is 45 m s^{-1}, impact angle 60°.

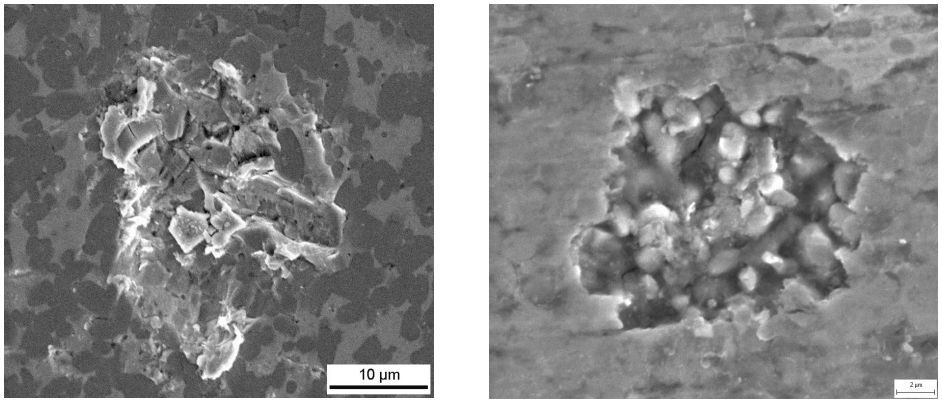

(a) (b)

Fig. 4. SEM micrographs of single impact craters produced in Cr_3C_2-30%Ni by a silica particles (a) and a silicon carbide particle (b).

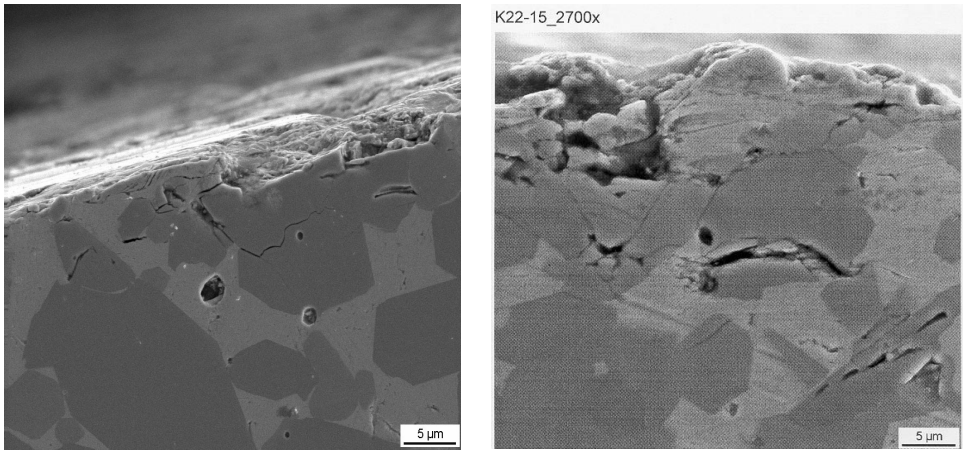

(a) (b)

Fig. 5. Subsurface cracks in a C2 sample.

If the erodent is much harder than the target material, crack initiation is inevitable and crack propagation is the controlling factor of the wear rate. The high volume fraction of carbides limits the plastic deformation that binder metal can absorb. This leads to more intensive carbide fracture, to matrix–grain debonding, and to hard grain fragmentation.

3.3. Erosion mechanism

During the erosion process the failure of the cermet material starts locally and in most cases, in the binder phase [1]. Carbide grains lose their protective binder and the eroded surface is almost entirely covered with the exposed carbides. Further processes depend on the hardness ratio of the target and erodent. Figure 6 shows the wear surfaces generated during the erosion test. In all cases the basic mechanism of wear is plastic deformation combined with brittle fracture. The degree of fracture correlates directly with the wear resistance of the hard carbide particles [7]. However, the wear rate of non-homogeneous materials can be hardly evaluated by conventionally measured mechanical properties of bulk materials [8]. Table 2 shows erosion rates of some cerments. Hardness H is usually accepted to be the best indicator of wear resistance. Materials with a higher hardness (or hard phase content) are assumed to be more wear resistant. However, such predictions are not supported by this study. The relative ranking of the materials investigated with respect to erosion rate could be explained by their different microstructures, whereas hardness of cermets seems to be of minor importance.

Since the erosion of brittle grains takes place primarily via a mechanism involving the initiation and propagation of microcracks, one expects that the fracture toughness of the material will affect the erosion rate [1,9]. In an attempt to rank materials on the basis of their intrinsic properties, several models have been

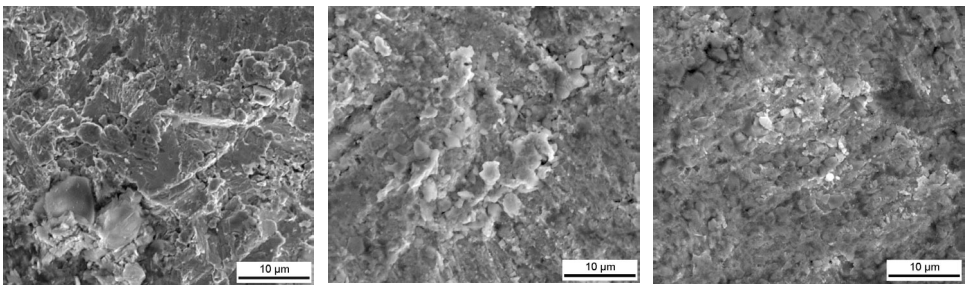

(a) (b) (c)

Fig. 6. SEM micrographs of the eroded surfaces impacted by silica particles at impact angle 60° and impact velocity 45 m s^{-1}: (a) C2; (b) BS2; (c) B2.

Table 2. Mechanical properties and erosion rate of some cermets

Grade	Vickers hardness *HV*	$K_{IC}^{-1.3} H^{-0.25} \times 10^3$	Erosion rate, $mm^3\ kg^{-1}$	
			Erodent – SiO_2	Erodent – SiC
A1	1350	5.88	1	75
BS1	1320	4.9	8	90
B1	1378	6.86	5.5	110
C1	1410	8.4	6	150

developed, which assume that subsurface lateral fracture is responsible for much of the material removed during the erosive wear [10,11]. For fixed particle and test parameters, the erosion rate of the target materials can generally be expressed as

$$E = C\, K_{IC}^{m}\, H^{n} = C\, \zeta,$$

where the exponents m and n have a negative value and C is a constant of proportionality. Evans et al. [10] proposed to use $m = -1.3$ and $n = -0.25$. Assuming that all environmental factors are constant, the volume wear of various grades should be controlled by the overall magnitude of ζ, with low values of ζ predicting lower wear rates.

For the investigation of the solid particle erosion of composites, a conventional centrifugal four-channel accelerator was used [11].

The data on the cermets, examined in this study, show that our approach does not provide a consistent correlation between the erosion rate and ζ, as it is apparent from Table 2. One possible reason for this may be that in these materials the lateral fracture is not the predominant fracture mechanism and material removal in an erosive environment results from a combination of three processes: plastic deformation of the binder (Fig. 6), transgranular subsurface fracture (Figs. 5 and 7), and intergranular fracture and/or displacement of carbide grains (Fig. 7). The mechanism depends on microstructural characteristics of the material which influence plastic deformation and brittle fracture. For example, a

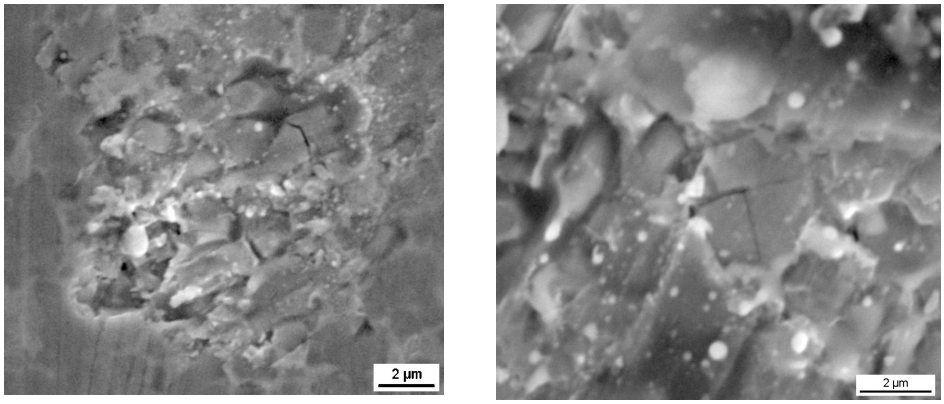

(a) (b)

Fig. 7. Cracking at the impact side.

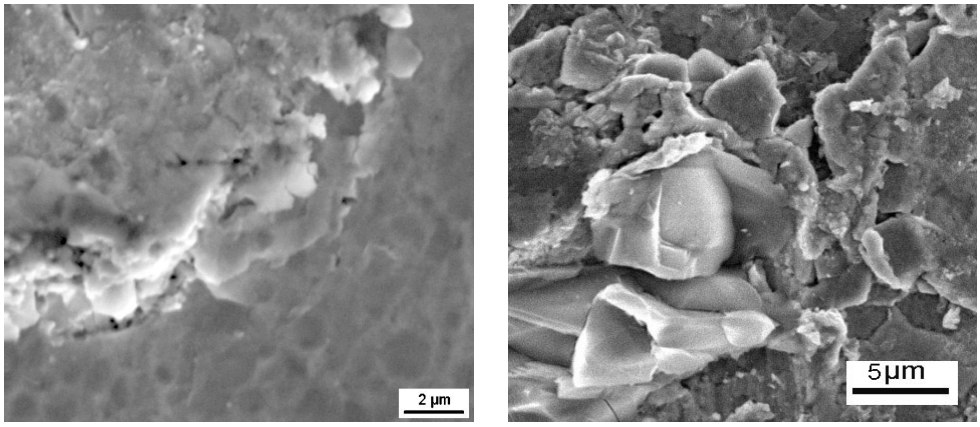

(a) (b)

Fig. 8. (a) Transgranular and grain–binder cracking near the impact side on the surface of a B2 sample; (b) silica particle debris embedded in the surface of a C2 sample.

high performance of WC-Co cermets may be attributed to a toughness of carbide grains that is high enough to withstand contacts with high amounts of dissipated energy without microfracture [12]. In contrast to the tough WC particles, TiC and Cr_3C_2 grains are very brittle (fracture toughness of about 3 MPa $m^{1/2}$) [13].

During erosion the non-homogeneous materials perform differently. The chromium carbide particles undergo increasing intergranular fragmentation below the wear surface while titanium carbide particles mostly undergo intra-granular cracking on the surface (Fig. 8a). As a result, the depth of deformation in the case of chromium carbide based composites is higher than in the TiC- or WC-based alloys.

It should also be noticed that a mechanically mixed layer may be formed on a composite surface during erosion testing. It consists not only of matrix carbide particles and binder metal but also of nanometer-scaled particles of the erodent debris. Figure 8b shows a silica particle embedded in the surface of a C2 sample.

4. CONCLUDING REMARKS

The results of this study suggest that microstructural variables influence the wear behaviour. These factors are not limited to matrix grain size and porosity but also include binder chemistry, grain boundary structure and, although not underlined in this work, thermal expansion mismatch stresses created by the sintering process. Since the coefficients of thermal expansion of the constituent phases are usually quite dissimilar, cooling from the high fabrication and processing temperatures to room temperature almost always generates high enough thermal stresses for the onset of local viscoplastic deformation. Additional inelastic deformation may be generated by mechanical pressure applied during fabrication. Together with the stresses imposed by mechanical loads, composite materials support residual stresses due to eigenstrains or transformation strains in the constituents. The magnitudes of stresses vary, but may be quite substantial to cause internal damage either alone or in superposition with the mechanical stresses. Therefore, these characteristics should be taken into consideration in any discussion of the tribological performance of the bulk materials.

It is believed that the improvement of the wear resistance is mainly due to the increase of the interphase bond strength and to the decrease of the number of microstructural flaws which are stress concentrators needed for nucleation and propagation of cracks, resulting in the removal of the materials. Strong interfacial bonding between constituent phases will prevent the pull-out of hard particles during erosion.

The composition of binder phase determines whether the stresses at the boundary are tensile or compressive and thus determines whether fracture of the material is transgranular or intragranular. Residual stresses that promote coherence of interfaces should be generated where possible. The fabrication methods need to be modelled and controlled to minimize the density of pre-existing flaws and to improve the initial stress state.

Behaviour of the non-homogeneous materials cannot be evaluated only by a measured mechanical characteristic or by a complex of the bulk properties. First of all, the stress state should be taken into account. Secondly, the internal state of the multiphase material depends on its microstructural characters.

Therefore for the evaluation of the tribological performance of the particle reinforced composites, fabrication methods and structure defects obtained during fabrication, including porosity, wettability, cooling temperature, etc. as well as microstructural effects must be taken into consideration.

ACKNOWLEDGEMENT

This work was supported by the Estonian Science Foundation (grant No. 5015).

REFERENCES

1. Hussainova, I., Pirso, J., and Kübarsepp, J. Mechanical properties and features of erosion of cermets. *Wear*, 2001, **250**, 818–825.
2. Chermant, J., Deschanvres, A., and Osterstock, F. Abrasive wear of brittle solids. *Powder Met*., 1977, **20**, 63–69.
3. Kenneth, J. and Brooks, J. *Hardmetals and Other Hard Metals*. Int. Carbide Data, ASM International, USA, 1992.
4. Hines, J., Bradt, R. C., and Biggers, J. Grain size and porosity effects on the abrasion wear of ceramics. *J. Am. Ceram. Soc*., 1995, **78**, 881–891.
5. Evans, A. and Charles, E. Wear mechanisms in ceramics. *J. Am. Ceram. Soc*., 1979, **62**, 371–382.
6. Larssen-Basse, J. Effect of composition, microstructure and service conditions on the wear of cemented carbides. *J. Metals*, 1983, November, 35–41.
7. Hussainova, I. Some aspects of solid particle erosion of cermets. *Tribology Int*., 2001, **34**, 89–93.
8. Hussainova, I. Microstructural aspects on wear of nonhomogeneous materials. In *Proc. World Congress on Powder Metallurgy*. Orlando, Florida, 2002, CD-ROM.
9. Doğan, C. and Hawk, J. Role of composition and microstructure in the abrasive wear of high-alumina ceramics. *Wear*, 1999, **225–229**, 1050–1058.
10. Evans, A., Golden, M., and Rosenblatt, M. Impact damage in brittle materials. *Proc. Roy. Soc. London Ser. A*, 1978, **A361**, 343–353.
11. Ruff, A. and Wiederhorn, S. Erosion by solid particle impact. In *Treatise on Materials Science and Technology* (Herman, H., ed.), Academic Press, NY, 1979, Vol. 16, 69–126.
12. Engqvist, H., Axen, N., and Hogmark, S. Tribological properties of a binderless carbide. *Wear*, 1999, **232**, 147–162.
13. Bondar, A., Masljuk, B., Velikanova, T., and Grytsiv, A. Phase diagram of Cr-Ni-C system. *Poroshkovaya Metallurgiya*, 1997, **5–6**, 13–24 (in Russian).

Mikrostruktuuri mõju mittehomogeensete materjalide kulumisele

Irina Hussainova ja Mart Viljus

Skaneeriva elektronmikroskoopia ja röntgenmikroanalüüsi abil on uuritud WC, TiC ja Cr_3C_2 baasil valmistatud kermiste mikrostruktuuri mõju nende sulamite triboloogilistele omadustele. Harilikult peetakse materjali kulumiskindlust otseselt sõltuvaks eelkõige tema kõvadusest ja jäetakse tähelepanuta mikrostruktuuri mõju. Artiklis on näidatud, et sama kõvadusega kermiste kulumiskiirus võib erineda mitmeid kordi. Selle nähtuse põhjuseid tuleb otsida materjalide koostisest ja mikrostruktuurist – karbiidi ja sideaine vahekorrast, karbiiditerade suurusest ja kujust, struktuuridefektidest, sisepingetest ja teistest teguritest. Kermiste kulumiskindlust on võimalik tõsta karbiidi ja sideaine vahelise sideme tugevdamise ning poorsuse ja muude sisedefektide vähendamise teel.